

Optical properties of self assembled GaN polarity inversion domain boundary

M.-C. Liu, Y.-J. Cheng, J.-R. Chang, S.-C. Hsu, and C.-Y. Chang

Citation: *Appl. Phys. Lett.* **99**, 021103 (2011); doi: 10.1063/1.3610449

View online: <http://dx.doi.org/10.1063/1.3610449>

View Table of Contents: <http://apl.aip.org/resource/1/APPLAB/v99/i2>

Published by the [American Institute of Physics](#).

Related Articles

Enhancement of light extraction efficiency by evanescent wave coupling effect in ridge-shaped AlGaInP/GaInP quantum wells

Appl. Phys. Lett. **100**, 091107 (2012)

Compositional instability in InAlN/GaN lattice-matched epitaxy

Appl. Phys. Lett. **100**, 092101 (2012)

Interfacial chemistry in an InAs/GaSb superlattice studied by pulsed laser atom probe tomography

Appl. Phys. Lett. **100**, 083109 (2012)

Impact of the misfit dislocations on two-dimensional electron gas mobility in semi-polar AlGaIn/GaN heterostructures

Appl. Phys. Lett. **100**, 082101 (2012)

Molecular beam epitaxy of InAlN lattice-matched to GaN with homogeneous composition using ammonia as nitrogen source

Appl. Phys. Lett. **100**, 072107 (2012)

Additional information on *Appl. Phys. Lett.*

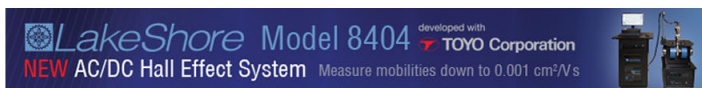
Journal Homepage: <http://apl.aip.org/>

Journal Information: http://apl.aip.org/about/about_the_journal

Top downloads: http://apl.aip.org/features/most_downloaded

Information for Authors: <http://apl.aip.org/authors>

ADVERTISEMENT



Optical properties of self assembled GaN polarity inversion domain boundary

M.-C. Liu,¹ Y.-J. Cheng,^{1,a)} J.-R. Chang,² S.-C. Hsu,³ and C.-Y. Chang²

¹Research Center for Applied Sciences, Academia Sinica, Taipei 11529, Taiwan

²Institute of Electronics, National Chiao Tung University, 1001 Ta Hsueh Rd., Hsinchu 300, Taiwan

³Department of Chemical and Materials Engineering, Tamkang University, No.151, Yingzhuang Rd., Danshui Dist., Taipei, Taiwan

(Received 12 November 2010; accepted 23 June 2011; published online 13 July 2011)

We report the fabrication of GaN lateral polarity inversion heterostructure with self assembled crystalline inversion domain boundaries (IDBs). The sample was fabricated by two step molecular-beam epitaxy (MBE) with microlithography patterning in between to define IDBs. Despite the use of circular pattern, hexagonal crystalline IDBs were self assembled from the circular pattern during the second MBE growth. Both cathodoluminescent (CL) and photoluminescent (PL) measurements show a significant enhanced emission at IDBs and in particular at hexagonal corners. The ability to fabricate self assembled crystalline IDBs and its enhanced emission property can be useful in optoelectronic applications. © 2011 American Institute of Physics. [doi:10.1063/1.3610449]

III-Nitride semiconductors, in particular GaN, have attracted great research interests in past few years due to their promising applications for UV to blue optoelectronic devices.¹ One of the important properties of wurtzite GaN is its strong spontaneous and piezoelectric polarization, which can induce surface charges and create large internal electric field in the film. This electric field can strongly affect the electrical and optical properties of GaN based devices.^{2,3} It can reduce the electron-hole wave function overlap in quantum well devices and have adverse effect on its light emitting efficiency. The direction of internal field depends on crystal c-axis orientation, which is not symmetric. Conventionally, the surface in the positive and negative c-axis direction is labeled as Ga- (0001) and N-polar (000-1) surface, respectively.

Recently, there are interests in studying the physical property of inversion domain boundary between Ga- and N-polar regions. The inversion domain boundary (IDB) has been found to exist at microscopic scale in Ga-polar GaN thin film grown by molecular-beam epitaxy (MBE).⁴ The IDB can also be created by intentionally growing lateral polarity heterostructures, where patterned Ga- and N-polar regions are laterally grown on the same substrate to form IDBs.⁵⁻⁷ The ability to fabricate controlled polarity pattern can open up additional device design dimension and applications. The IDB has been studied theoretically,^{8,9} and experimentally imaged by high-resolution transmission electron microscope,^{4,5} and piezoelectric force microscope.^{10,11} It was theoretically predicted that IDBs in wurtzite GaN would not have electronic states in the band gap, implying that they would not affect photoluminescent (PL) efficiency.⁸ The optical property of IDB has been investigated by high-resolution spatially resolved PL measurement.¹² The measurement was done at 10 K low temperature and significantly brighter emission was reported at IDBs. However, the observed emission from IDB was neither spectrally nor spatially uniform. The nonuniformity could be due to the coexistence of differ-

ent crystalline planes in the intentionally patterned IDB, which was suggested possibly having mixed crystalline planes {10-10} and {11-20}. The fabricated IDB was a straight line in tens of μm and not oriented along any specific crystal plane. That could be the reason for leading to mixed crystalline planes in IDBs. The observed PL peaks have some variations and are about 30–40 meV lower than the bulk Ga-polar emission. A theoretical calculation however predicts a zero shift in emission peak at IDB.⁹ The discrepancy may come from the mixed crystal planes in IDBs and possible defects associated with them. The ability to fabricate crystalline IDB paves the way for better physical property study. It may also open up new applications due to its enhanced emission property.

Here we report the fabrication of self assembled IDB along {10-10} crystalline plane and the observation of enhanced light emission at IDB by cathodoluminescent (CL) and PL measurement. The crystalline IDBs were fabricated by two step rf-plasma-enhanced MBE, where microlithography patterning process was used in between two growth steps to define lateral polarity heterostructure boundary. Circular patterns were used in microlithography patterning process. However, hexagonal crystalline IDBs along {10-10} crystalline planes were self assembled from the original circular pattern after the second MBE re-growth. Both CL and PL measurements show an enhanced light emission at IDBs and a zero shift in emission peak.

It is known that GaN grown on c-plane sapphire by MBE normally has an N-polar surface. It has also been demonstrated that the polarity of GaN can be switched to Ga-polar surface by pre-growing a high temperature AlN buffer layer on c-plane sapphire surface. The fabrication steps, as shown in Figs. 1(a)–1(d), use these two growth techniques and microlithography patterning to grow patterned lateral polarity heterostructure. First, a high temperature (930 °C) thin AlN buffer layer (30 nm) was grown on top of a (0001) sapphire substrate followed by a thin layer of GaN growth (810 °C, 50 nm) [Fig. 1(a)]. Ga-polar GaN was grown on AlN buffer layer, which was confirmed by *in situ* (2×2)

^{a)}Author to whom correspondence should be addressed. Electronic mail: yjcheng@sinica.edu.tw.

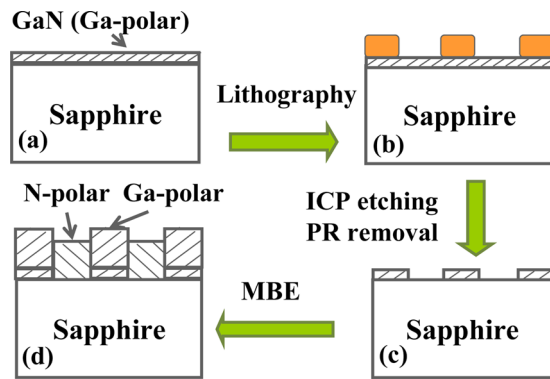


FIG. 1. (Color online) (a)–(d) Processing flow for fabricating patterned polarity IDB. (a) Grow Ga-polar GaN layer. (b) Photoresist patterning. (c) ICP etching to remove unmasked region followed by PR removal (d). The second growth to form polarity heterostructure.

reflection high energy electron diffraction (RHEED) pattern.^{13–15} Photoresist (PR) was then spun on the sample and patterned using microlithography to create $3\ \mu\text{m}$ circular mesa masks [Fig. 1(b)]. The sample was etched in an inductively coupled plasma (ICP) etcher using Ar/Cl₂ gas until the unmasked GaN regions were etched down to expose sapphire substrate surface. The PR mask was then removed, leaving $3\ \mu\text{m}$ circular Ga-polar GaN mesas on sapphire substrate [Fig. 1(c)]. The sample was subsequently reintroduced into the MBE system to grow $1\ \mu\text{m}$ ($810\ ^\circ\text{C}$) GaN layer. Since AlN buffer layer was removed by the etching process, the re-grown GaN on the exposed sapphire surface would be N-polar.¹³ The same second step growth parameter was applied to a separate blank sapphire substrate to verify that it did grow N-polar GaN, which was confirmed by *in situ* (3×3) RHEED pattern. The GaN grown on the circular Ga-polar GaN mesa, which worked as a seeding layer, will still follow the same Ga polarity direction. As a result, we obtained a patterned lateral polarity heterostructure with pre-defined IDBs.

A scanning electron microscope (SEM) plane view of the sample is shown in Fig. 2(a). It is interesting to observe the self assembly of hexagonal shapes after the second MBE growth even though circular pattern was originally used to define polarity inversion boundary. From the growth process design, the polarity inside hexagon is Ga-polar, while the surrounding area is N-polar. The IDBs were self assembled at $\{10\text{-}10\}$ hexagonal crystal planes. There have been reports showing the growth speeds of different crystalline planes in selective area lateral overgrowth on patterned oxide mask with circular openings.¹⁶ The observed growth rate of $(10\text{-}11)$ plane is much slower than that of (0001) plane. As a result, the selective lateral overgrowth often leads to a hexagonal boundary in the in-plane direction despite of the original circular pattern. In our experiment, it is a 2-D thin film growth instead of a 3-D lateral overgrowth. As a result, IDBs are self-assembled at $\{10\text{-}10\}$ hexagonal planes. The SEM was switched to cathodoluminescent detection under the same magnification condition. The CL image is shown in Fig. 2(b). The focused e-beam spot size is less than $10\ \text{nm}$, which defines the CL imaging spatial resolution. The cathodoluminescent intensity is significantly stronger at IDBs and maximum at hexagonal corner. The luminescent intensity at

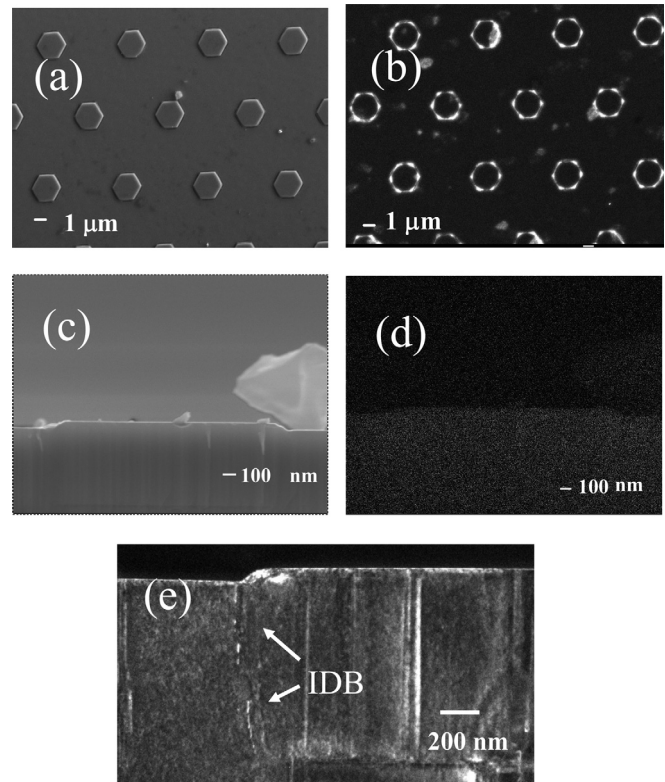


FIG. 2. (a) SEM plane view image of the sample surface. (b) CL image at the same magnification showing the enhanced luminescent intensity at IDBs. (c) SEM cross section image. (d) CL image. (e) TEM cross section view.

IDB gradually decreases with position moving away from corner along the boundary. A SEM cross section and CL images are shown in Figs. 2. It shows that the hexagonal Ga-polar region is about $80\ \text{nm}$ higher than the surrounding N-polar surface, which is consistent with the thickness of Ga-polar seeding layer. The cross section profile shows a slow inclined side wall of about $160\ \text{nm}$ at IDBs. The cross section CL does not show visible enhancement as the plane view CL does, neither at the IDBs nor the IDB mesa edge. This might indicate that the enhancement is a shallow surface effect on c-plane and requires further investigation. A cross section TEM picture is shown in Fig. 2(e), which shows the IDB propagating from the edge of patterned AlN buffer layer to the top surface.

The plane view CL intensity spectra taken at the hexagonal corner (A), middle of hexagonal boundary (B), center of hexagonal Ga-polar region (C), and N-polar region (D) are shown in Fig. 3(a). The intensity magnitudes of these four points in descending order follow the same sequence.

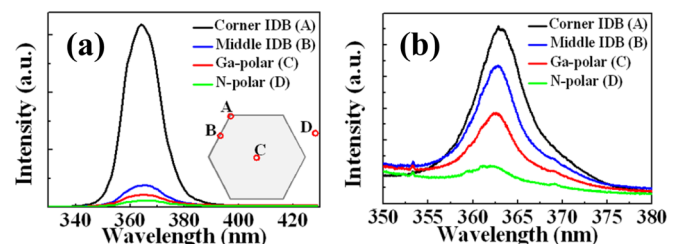


FIG. 3. (Color online) (a) CL intensity spectra at various sample locations. (b) PL intensity spectra at various sample locations.

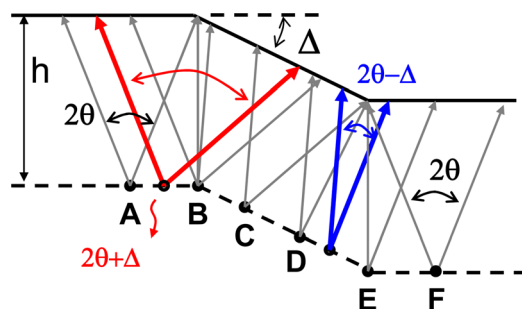


FIG. 4. (Color online) Escape light cone analysis around IDB.

The full width at half maximum (FWHM) linewidth is about 14 nm for all spectra. The intensity at Ga-polar region is significantly higher than that at N-polar region. Ga-polar GaN is known to have better material quality than N-polar GaN, which explains the observed higher luminescent intensity. The intensity at IDB, in particular at the hexagonal corner, is much higher than both Ga- and N-polar region. The peak wavelength of the enhanced luminescence at IDB is the same as those for Ga- and N-polar GaN, consistent with the theoretical prediction.¹² This is in contrast to the 30 meV redshift reported from IDB with mixed crystal planes where the redshift could be due to shallow defect traps created among the mixed crystal planes. The PL spectra of the sample were also measured using 325 nm He-Cd laser pumping source. The laser was focused on the sample by a $39\times$ UV objective with a focused spot size of 0.8 μm . The PL spectra at similar locations are shown in Fig. 3(b). It reconfirms the enhanced light emission at IDBs. The relative intensity magnitudes at different locations are similar to the CL case except that the intensity at corner is not as strong. This is likely due to the area average effect of the much larger excitation source spot size in PL measurement and implies that the great enhancement is localized to a very small region. A theoretical model based on *ab initio* density functional calculation has shown that the electronic potential tends to trap electrons and holes in the IDB vicinity.⁹ This could provide better e-h recombination efficiency and explain the enhanced emission. However, the inclined surfaces at IDBs, as shown in Fig. 2(c), may provide better light extraction and contribute to the observed enhanced emission as well.

To estimate the light extraction effect, we analyze the escape light cones using a simplified ray model as shown in Fig. 4, where point source locations are shown in dotted line. The surface inclined angle Δ is about 26.5° from SEM cross section. The total internal reflection angle θ is 24° from GaN refractive index of 2.45. Each point source has two rays defining the escape light cone (ELC). For all the points to the left of point A, the ELC is the nominal 2θ value. For points between A and B, ELC has its maximum value $2\theta+\Delta$. For points between B and C, it is back to 2θ . Going further from point C to D, ELC decreases from 2θ to θ . For points between D and E, ELC is at minimum value of $2\theta-\Delta$. ELC then increases from θ at point E to 2θ at point F. From the analy-

sis, we see that the upper bound of light extraction enhancement is $(2\theta+\Delta)/2\theta=55\%$ occurring for points between A and B. This is still smaller than the observed 75% CL emission enhancement at the middle of IDB, compared to Ga-polar region. This indicates that even though light extraction makes significant contribution to the observed enhanced emission, the material property at IDBs also contribute to a significant portion of enhancement. The much brighter emission at IDB corners could be due to the sharp turning angle, which may increase light extraction by scattering the waveguide mode guided along the IDB into free space.

In summary, the fabrication of polarity inversion GaN heterostructure with self assembled $\{10\text{-}10\}$ crystal plane IDBs is demonstrated. The fabrication process involves two step rf-enhanced MBE growths and lithography patterning in between two growths to define IDBs. Despite the use of circular patterns for defining IDBs, hexagonal crystalline IDBs are self assembled from the original circular patterns in the second epitaxial growth. CL and PL measurements show that luminescent property is significantly enhanced at IDBs. The ability to fabricate crystalline IDB and the demonstration of its enhanced luminescent property offers an additional device design dimension and could be of useful in GaN based light emitting devices.

This work was financially supported by Sinica Nano-program and in part by the National Science Council of Republic of China (ROC) Taiwan under contract NSC97-2112-M-001-027-MY3 and Sinica Nano Program.

¹T. Mukai, K. Takekawa, and S. Nakamura, *Jpn. J. Appl. Phys. Part 2* **37**, L839 (1998).

²O. Ambacher, J. Smart, J. R. Shealy, N. G. Weimann, K. Chu, M. Murphy, R. Dimitrov, L. Wittmer, M. Stutzmann, W. Rieger, and J. Hilsenbeck, *J. Appl. Phys.* **85**, 3222 (1999).

³M. Stutzmann, O. Ambacher, M. Eickhoff, U. Karrer, A. Lima Pimenta, R. Neuberger, J. Schalwig, R. Dimitrov, P. Schuck, and R. Grober, *Phys. Status Solidi B* **288**, 505 (2001).

⁴C. Iwamoto, X. Q. Shen, H. Okumura, H. Matuhata, and Y. Ikuhara, *Appl. Phys. Lett.* **79**, 3941 (2001).

⁵F. Liu, R. Collazo, S. Mita, Z. Sitar, G. Duscher, and S. J. Pennycook, *Appl. Phys. Lett.* **91**, 203115 (2007).

⁶S. Pezzagna, P. Vennéguès, N. Grandjean, A. D. Wieck, and J. Massies, *Appl. Phys. Lett.* **87**, 062106 (2005).

⁷A. Chowdhury, H. M. Ng, M. Bhardwaj, and N. G. Weimann, *Appl. Phys. Lett.* **83**, 1077 (2003).

⁸J. E. Northrup, J. Neugebauer, and L. T. Romano, *Phys. Rev. Lett.* **77**, 103 (1996).

⁹V. Fiorentini, *Appl. Phys. Lett.* **82**, 1182 (2003).

¹⁰B. J. Rodriguez, A. Gruverman, A. I. Kingon, R. J. Nemanich, and O. Ambacher, *Appl. Phys. Lett.* **80**, 4166 (2002).

¹¹R. Katayama, Y. Kuge, K. Onabe, T. Matsushita, and T. Kondo, *Appl. Phys. Lett.* **89**, 231910 (2006).

¹²P. J. Schuck, M. D. Mason, R. D. Grober, O. Ambacher, A. P. Lima, C. Miskys, R. Dimitrov, and M. Stutzmann, *Appl. Phys. Lett.* **79**, 952 (2001).

¹³X. Q. Shen, T. Ide, S. H. Cho, M. Shimizu, S. Hara, and H. Okumura, *Appl. Phys. Lett.* **77**, 4013 (2000).

¹⁴D. Huang, P. Visconti, K. M. Jones, M. A. Reshchikov, F. Yun, A. A. Baski, T. King, and H. Morkoc, *Appl. Phys. Lett.* **78**, 4145 (2001).

¹⁵A. R. Smith, R. M. Feenstra, D. W. Greve, M.-S. Shin, M. Skowronski, J. Neugebauer, and J. E. Northrup, *Appl. Phys. Lett.* **72**, 2114 (2001).

¹⁶B. Beaumont, S. Haffouz, and P. Gibart, *Appl. Phys. Lett.* **72**, 1227 (1998).